Journal of Applied Mechanics and Technical Physics, Vol. 47, No. 5, pp. 696–703, 2006

ON THE THRESHOLD FORCE PULSES FOR SPALL FRACTURE OF MATERIALS

V. I. Smirnov

UDC 539.3

Spall fracture is considered using the classical one-dimensional model. Results of the analysis are used to predict the dynamic strength properties of some structural materials, in particular, rail steels. The dependence of the time of fracture of the material on the threshold amplitude and time of loading is obtained. A model for the comparative estimation of the dynamic strength of materials is proposed, and corresponding diagrams are constructed. It is shown that the fracture process can be optimized by choosing the duration of loading of the material.

Key words: *spall, time dependence of strength, threshold load pulse, structure–time criterion.*

Introduction. The traditional strength concepts and the methods of testing the mechanical properties of materials and structures are inefficient for describing the processes occurring under intense high-speed loading conditions. To analyze the high-speed operation of various structures, one needs new fracture criteria for solids that are capable of adequately describing the process of dynamic fracture of materials.

Spall testing of solids is one of the most important experiments intended to determine the dynamic strength properties of structural materials.

In the present paper, we study the threshold spall-strength characteristics of some rail steels for the purpose of developing new computational methods for solving safety problems for high-speed transport systems.

1. Time Dependence of Strength. We consider the spall fracture using the traditional modeling scheme [1]. The first attempts to analyze spall were based on using the critical stress criterion

$$\sigma \le \sigma_c \tag{1.1}$$

(σ_c is the static strength of the material). Experiments have shown that this criterion does not explain a number of features of spall fracture, in particular, the time dependence of strength and the spatial distribution of fracture [1].

To explain some phenomena observed in experiments, such as the occurrence of the dynamic branch and the formation of an extended cavitation zone, Nikiforovskii and Shemyakin [1] proposed the time criterion

$$\int_0^{t_*} \sigma(t)\,dt \leqslant J_c \tag{1.2}$$

(J_c is the critical pulse). This criterion, which is used to analyze the fracture caused by very short loading pulses, allows one to substantiate many important spall characteristics, in particular, to explain an increase in material strength (critical rupture stress) with increasing loading rate. However, results of experiments and fractographic analysis of fracture indicate that this process is significantly affected by structure. Accounting for the structural features of fracture provides new information on the time dependence of material strength, whose explanation and theoretical description remains an urgent problem. At the same time, complicated physical theories of fracture that take into account structural processes are not always effective for solving practical engineering problems. Therefore, it is expedient to develop simpler methods that take into account the basic features of dynamic fracture.

Petersburg State University of Means of Communication, St. Petersburg 198103; mirnov@VS13866.spb.edu.
Translated from Prikladnaya Mekhanika i Tekhnicheskaya Fizika, Vol. 47, No. 5, pp. 97–106, September–October, 2006. Original article submitted October 29, 2005.

As such an approach, Morozov and Petrov [2] proposed a structure–time criterion that takes into account the pulse characteristics of stress fields and the structural features of materials. In the case of "faultless" media (in particular, for spall), it has the form

$$\int\limits_{t-\tau}^{t} \sigma(s)\,ds \le \sigma_c\tau, \tag{1.3}$$

where τ is the incubation (structural) time of fracture.

We use relation (1.3) to analyze the spall fracture of samples of rail steels of different grades. We consider the reflection of a compressing stress pulse of a triangular shape (with regions of buildup and attenuation of the same duration t_0) from the free end a semi-infinite rod. The Ox axis is directed along the rod, which is on the right of the coordinate origin ($x > 0$). The expression for the incident pulse is written as

$$\sigma_-(x,t) = -P\Big[\frac{ct+x}{ct_0}\,[H(ct+x) - H(ct+x-ct_0)]$$

$$+\Big(2-\frac{ct+x}{ct_0}\Big)[H(ct+x-ct_0) - H(ct+x-2ct_0)]\Big].$$

Here P is the pulse amplitude, c is the sound speed in the material, $2t_0$ is the sound duration, and $H(t)$ is a Heaviside function. After the reflection from the free end, the stress profile has the form

$$\sigma_+(x,t) = P\Big[\frac{ct-x}{ct_0}\,[H(ct-x) - H(ct-x-ct_0)]$$

$$+\Big(2-\frac{ct-x}{ct_0}\Big)[H(ct-x-ct_0) - H(ct-x-2ct_0)]\Big].$$

The total stress is equal to $\sigma(x,t) = \sigma_-(x,t) + \sigma_+(x,t)$.

An analysis of the behavior of $\sigma(x,t)$ shows that the first maximum of the tensile stress arises at the point $x_0 = ct_0/2$. We introduce the dimensionless quantities $T = t/\tau$ and $T_0 = t_0/\tau$. Then,

$$\sigma(T)\Big|_{x=x_0} = F(T) + G(T),$$

$$F(T) = -P\Big\{\Big(\frac{1}{2}+\frac{T}{T_0}\Big)\Big[H\Big(T+\frac{T_0}{2}\Big) - H\Big(T-\frac{T_0}{2}\Big)\Big]$$

$$+\Big(\frac{3}{2}-\frac{T}{T_0}\Big)\Big[H\Big(T-\frac{T_0}{2}\Big) - H\Big(T-\frac{3T_0}{2}\Big)\Big]\Big\},$$

$$G(T) = P\Big\{\Big(\frac{T}{T_0}-\frac{1}{2}\Big)\Big[H\Big(T-\frac{T_0}{2}\Big) - H\Big(T-\frac{3T_0}{2}\Big)\Big]$$

$$+\Big(\frac{5}{2}-\frac{T}{T_0}\Big)\Big[H\Big(T-\frac{3T_0}{2}\Big) - H\Big(T-\frac{5T_0}{2}\Big)\Big]\Big\}.$$

The threshold (minimum) fracture amplitude P_* at the specified time t_0 is found from the condition [according to criterion (1.3)]

$$\max_T I(T) = \sigma_c, \qquad I(T) = \int\limits_{T-1}^{T} \sigma(s)\,ds. \tag{1.4}$$

Integrating $\sigma(T)$ over T, we obtain

$$I_-(T) = \int\limits_{T-1}^{T} F(s)\,ds = -\frac{PT_0}{2}\Big\{[f_1(T) - f_1(T-1)] - [f_2(T) - f_2(T-1)] + f_3(T)\Big\},$$

$$f_1(T) = \Big(\frac{1}{2}+\frac{T}{T_0}\Big)^2\Big[H\Big(T+\frac{T_0}{2}\Big) - H\Big(T-\frac{T_0}{2}\Big)\Big],$$

$$f_2(T) = \Big(\frac{3}{2} - \frac{T}{T_0}\Big)^2 \Big[H\Big(T - \frac{T_0}{2}\Big) - H\Big(T - \frac{3T_0}{2}\Big)\Big],$$

$$f_3(T) = 2H\Big(\frac{T_0}{2} - T + 1\Big)H\Big(T - \frac{T_0}{2}\Big),$$

$$I_+(T) = \int\limits_{T-1}^{T} G(s)\,ds = \frac{PT_0}{2}\Big\{[g_1(T) - g_1(T-1)] - [g_2(T) - g_2(T-1)] + g_3(T)\Big\},$$

$$g_1(T) = \Big(\frac{1}{2} - \frac{T}{T_0}\Big)^2 \Big[H\Big(T - \frac{T_0}{2}\Big) - H\Big(T - \frac{3T_0}{2}\Big)\Big],$$

$$g_2(T) = \Big(\frac{5}{2} - \frac{T}{T_0}\Big)^2 \Big[H\Big(T - \frac{3T_0}{2}\Big) - H\Big(T - \frac{5T_0}{2}\Big)\Big],$$

$$g_3(T) = 2H\Big(\frac{3T_0}{2} - T + 1\Big)H\Big(T - \frac{3T_0}{2}\Big),$$

$$I(T) = I_-(T) + I_+(T).$$

An analysis of the function $I(T)$ shows that

$$\max_T I(T) = \begin{cases} I(3T_0/2 + 2/3), & T_0 \geq 2/3, \\ I(T_0 + 1), & T_0 \leq 2/3, \end{cases}$$

i.e., the time to fracture is equal to

$$T_* = \begin{cases} 3T_0/2 + 2/3, & T_0 \geq 2/3, \\ T_0 + 1, & T_0 \leq 2/3. \end{cases} \tag{1.5}$$

For such values of the argument, the maximum of the function $I(T)$ is reached:

$$\max_T I(T) = I(T_*) = \begin{cases} P(1 - 1/(3T_0)), & T_0 \geq 2/3, \\ 3PT_0/4, & T_0 \leq 2/3. \end{cases} \tag{1.6}$$

The time to fracture T_* as a function of the threshold amplitude P_* can be obtained from relation (1.4) using condition (1.5):

$$T_* = \begin{cases} 1/(2(1 - \sigma_c/P_*)) + 2/3, & 1 \leq P_*/\sigma_c \leq 2, \\ 4\sigma_c/(3P_*) + 1, & P_*/\sigma_c \geq 2. \end{cases} \tag{1.7}$$

Relation (1.7) between the time to fracture T_* (or in dimensional form, $t_* = T_*\tau$) and the threshold amplitude P_* is the time dependence of strength. Figure 1 gives a curve of (1.7) for V95 aluminum alloy and results of spall fracture experiments [3].

The dynamic strength is not a material constant but it depends on the time to fracture ("lifetime" of the sample). The introduction of the incubation time τ allows one to plot a unified curve of the time dependence of strength: the static branch (vertical asymptote in Fig. 1) and the dynamic branch (horizontal asymptote) are connected by a smooth transition. We note that the critical stress criterion (1.1) describes only the static branch, and criterion (1.2) only the dynamic branch. The time dependence of strength was first experimentally obtained in [3, 4] and analyzed in [5, 6] and other papers.

From an analysis of the time dependence of strength, one can infer the relationship between that the quasistatic and dynamic mechanisms of spall fracture and the ranges in which they are manifested. The spall strength is characterized by the obtained dependence $P_*(t_*)$ (see Fig. 1), on which the dynamic branch determined by the structural characteristic τ correspond to the dynamic fracture mechanism. The position of the dynamic branch does not depend on the static strength of the material σ_c, which is supported by experimental data. The transition zone corresponds to a joint manifestation of the dynamic and quasistatic fracture mechanisms. In this zone, the fracture threshold depends on both the dynamic fracture parameter τ and the static strength of the material. The static branch is completely determined by the static strength limit of the material σ_c.

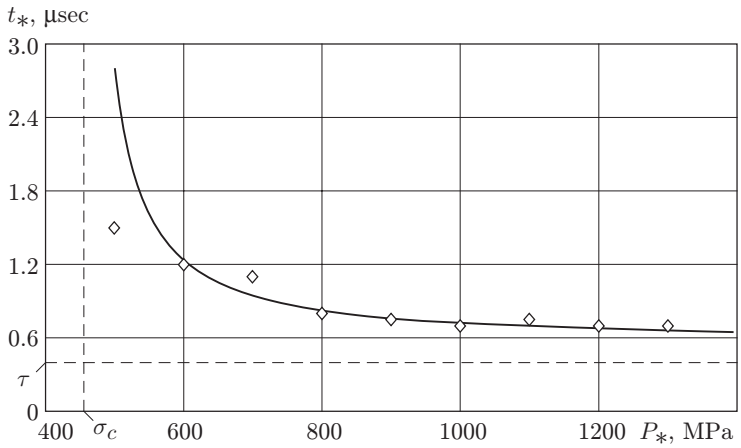

Fig. 1. Strength of V95 aluminum alloy versus time ($\sigma_c = 456$ MPa and $\tau = 0.45$ μsec): the solid curve is calculated using formula (1.7); the points are the experimental data of [3]; the vertical dashed curve is the asymptote of the static branch; the horizontal dashed curve is the asymptote of the dynamic branch.

TABLE 1

Steel grade (profile)	σ_c, MPa	K_{1c}, MPa · m$^{1/2}$	d, mm	τ, μsec	Reference
RS1400 (RZhD)	1452	43.0	0.56	0.11	[7]
1100 CrSiV (136RE)	1173	37.9	0.67	0.13	[8]
900 CrSiV (EB50)	1051	37.0	0.79	0.15	[8]
CHHR (132RE)	1265	46.0	0.84	0.16	[8]
900B (A65)	964	39.5	1.07	0.21	[8]
900ASTM (MRS67)	901	40.0	1.25	0.24	[8]
75G (RZhD)	1080	50.0	1.36	0.26	[9]
RS600 (RZhD)	680	40.0	2.20	0.42	[10]
RS700 (RZhD)	740	46.0	2.46	0.47	[10]
700 (MSZhD60)	777	70.0	5.17	1.00	[8]

Relations (1.5) allow one to establish the physical meaning of the incubation time considered. We write (1.5) in dimensionless form

$$t_* = \begin{cases} 3t_0/2 + 2\tau/3, & t_0 \geq 2\tau/3, \\ t_0 + \tau, & t_0 \leq 2\tau/3. \end{cases} \tag{1.8}$$

From the second expression in (1.8), it follows that $t_* \to \tau$ as $t_0 \to 0$. Thus, the incubation time τ is the time to fracture of the sample t_* under loading by a threshold pulse of infinitesimal duration (i.e., a pulse in the form of a Dirac delta-function). At threshold loads (amplitudes P_*) of zero duration, the time to fracture cannot be smaller than τ. The time to fracture can be smaller than the incubation time only in the case of superthreshold loads, i.e., under overload impacts.

2. Threshold Force Fracture Pulses for Rail Steels. Below, we give results of dynamic strength calculations for some rail steels whose mechanical characteristics are given in Table 1.

The incubation time τ is determined from experiments. In the absence of experimental data, the quantity τ can be approximately determined from the relation $\tau = d/c$ [2]. Results of calculations using this relation are in good agreement with experimental results [4] obtained in a certain range of the determining space–time parameters. Here $d = 2K_{1c}^2/(\pi\sigma_c^2)$ is the structural fracture parameter, K_{1c} is the static fracture viscosity, c is the maximum speed of elastic waves (in this case, $c = \sqrt{E/\rho}$, where E is the elastic modulus and ρ is the density of the material; for rail steel, $E = 0.21 \cdot 10^6$ MPa and $\rho = 7800$ kg/m^3). The incubation times τ calculated by the relation given above are presented in Table 1.

Figure 2 gives calculated time dependences of strength for three grades of rail steels. Although RS1400 (RZhD) steel has the highest quasistatic fracture strength, its strength under high-speed impact loading is lower

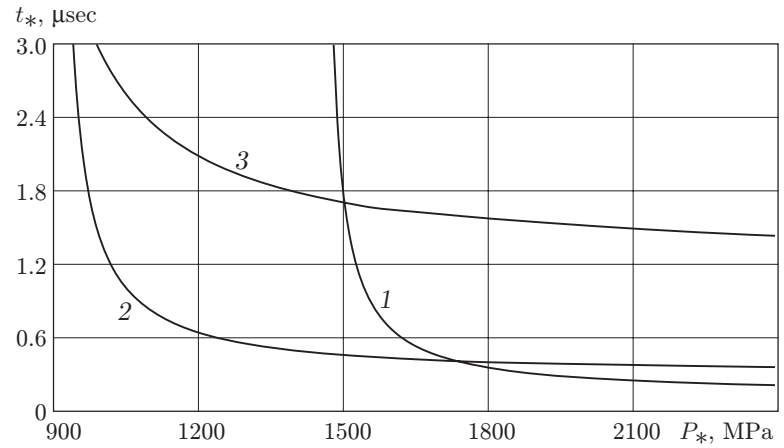

Fig. 2. Time dependences of strength for some grades of rail steels: 1) RS1400 (RZhD), 2) 900ASTM (MRS67), and 3) 700 (MSZhD).

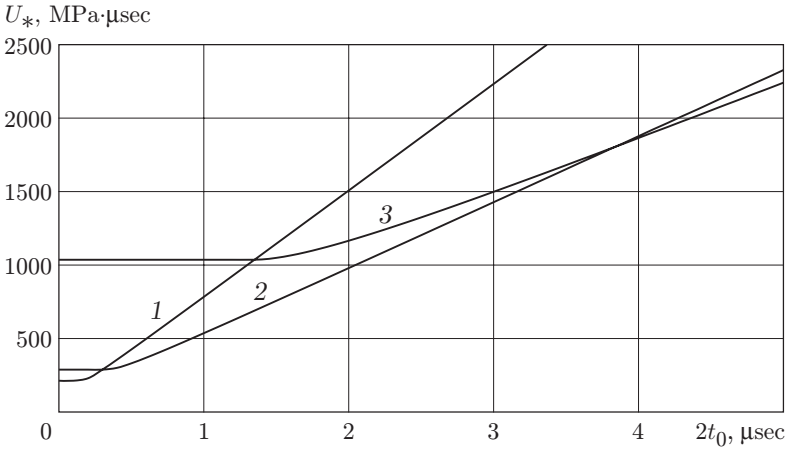

Fig. 3. Threshold fracture pulse for some grades of rail steels (notation the same as in Fig. 2).

than that of 700 (MSZhD) steel. This is due to the lower fracture resistance. Generally, however, it is difficult to compare the strength characteristics of various materials using the time dependence of strength: the material can have a higher threshold amplitude P_* than other materials but a small fracture time t_*, and vice versa (the parameters P_* and t_* are functions of the pulse duration $2t_0$). In practice, it is expedient to use the dependence of a certain integrated strength characteristic on the independent (varying in experiment) variable $2t_0$. As such a characteristic one can use the threshold force pulse U_*. For the specified time profile (an isosceles triangle), this quantity is $U_* = P_* t_0$. From relations (1.4) and (1.6), we find the threshold amplitude P_* as a function of the time of increase (decrease) t_0 of the load:

$$P_* = \begin{cases} \sigma_c/(1-\tau/(3t_0)), & t_0 \geq 2\tau/3, \\ 4\sigma_c\tau/(3t_0), & t_0 \leq 2\tau/3. \end{cases}$$

Then, the threshold fracture pulse is equal to

$$U_* = \begin{cases} 3\sigma_c t_0^2/(3t_0-\tau), & t_0 \geq 2\tau/3, \\ 4\sigma_c\tau/3, & t_0 \leq 2\tau/3. \end{cases} \tag{2.1}$$

In (2.1), the first expression corresponds to the static branch and the second expression to the dynamic branch. The dependence of the threshold fracture amplitude on the pulse duration $U_*(2t_0)$ for three grades of rail steels is given in Fig. 3. It is evident that the larger the threshold force pulse U_* with a specified loading time $2t_0$, the

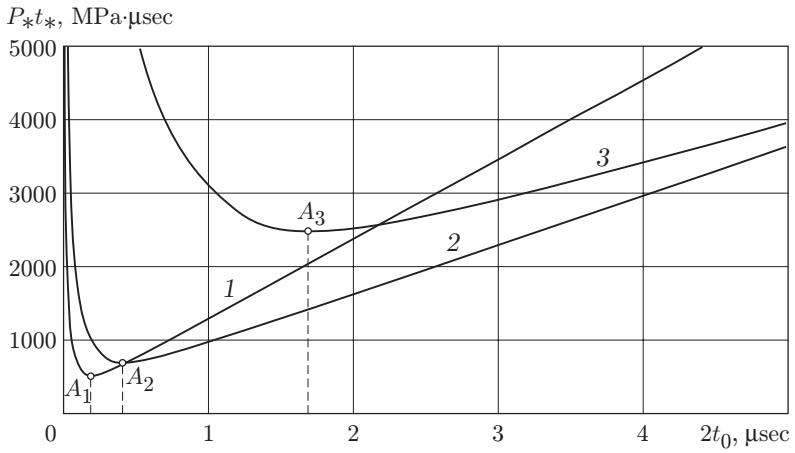

Fig. 4. The amount of fracture for some grades of rail steels (notation the same as in Fig. 2).

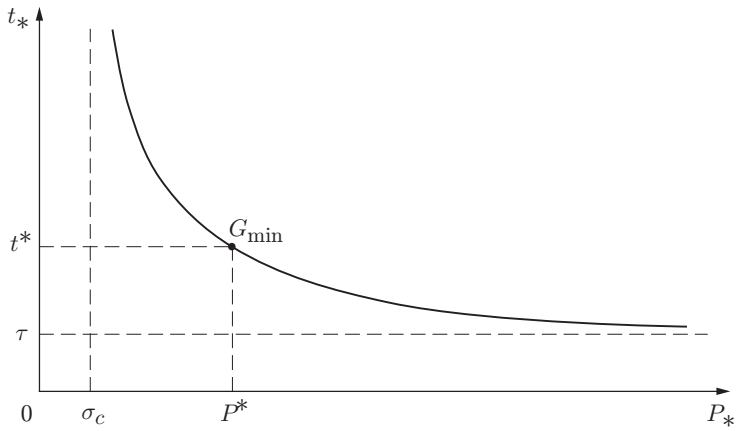

Fig. 5. Time dependence of strength in spall tests.

higher the dynamic strength of the rail steel, i.e., the higher its resistance to dynamic impact loading. Thus, for a loading time not exceeding 1.4 μsec, 700 (MSZhD) steel is the strongest of the three steels considered, and for loading times above 1.4 μsec, RS1400 (RZhD) steel is the strongest. 900ASTM (MRS67) steel is intermediate for $2t_0 < 0.3$ μsec and $2t_0 > 4$ μsec. In the range of loading times $0.3 < 2t_0 < 4.0$ μsec, it turns out to be the least strong.

Another limiting fracture characteristic is the product of the threshold fracture amplitude into the fracture time $G = P_*t_*$. In contrast to the threshold force fracture pulse, this quantity (we shall call it the amount of fracture) is not a classical physical characteristic, but in the problem in question, it is the most informative.

Figure 4 gives curves of the amount of fracture versus loading time for three grades of rail steels. We note that the indicated curves have a minimum (the points A_1, A_2, and A_3 in Fig. 4), which is due to the fact that as the loading time increases, the fracture time t_* increases whereas the threshold loading amplitude P_* decreases. This allows one to choose the loading time so as to achieve fracture of the material with minimum energy expenses. For example, for RS1400 (RZhD) steel, this loading time is 0.18 μsec, whereas for 700 (MSZhD) steel, it is 1.7 μsec. The minimum amount of fracture for these steels is $G_{\min} = 510.5$ and 2482.0 MPa $\cdot$ μsec, respectively. The optimum loading time $2t_0^{\text{opt}}$ and its corresponding minimum amount of fracture $G_{\min}$ for different rail steels are given in Table 2. For the optimum loading time, 700 (MSZhD) steel is the strongest of the steels considered and 1100 CrSiV (136RE) steel is the least strong.

According to theory [11], the minimum amount of fracture is equal to the fracture "quantum" $\sigma_c\tau$ (Fig. 5). In this case, the region of transition from quasistatic to dynamic loading and back on the curve of $P_*(t)$ is a point

TABLE 2

Grade of steel (profile)	$G_{\min}$, MPa $\cdot$ μsec	$2t_0^{\text{opt}}$, μsec
RS1400 (RZhD)	510.5	0.18
1100 CrSiV (136RE)	487.1	0.22
900 CrSiV (EB50)	503.6	0.25
CHHR (132RE)	646.5	0.27
900B (A65)	646.6	0.35
900ASTM (MRS67)	690.7	0.40
75G (RZhD)	896.9	0.44
RS600 (RZhD)	912.3	0.71
RS700 (RZhD)	1111.0	0.78
700 (MSZhD60)	2482.0	1.70

TABLE 3

Material	σ_c, MPa	K_{Ic}, MPa $\cdot$ m$^{1/2}$	E, GPa	ρ, kg/m^3	c, m/sec	τ, μsec
PMMA	70	1.47	2.45	1089	1500	32
AISI 4340	1490	50	208	7800	5165	7

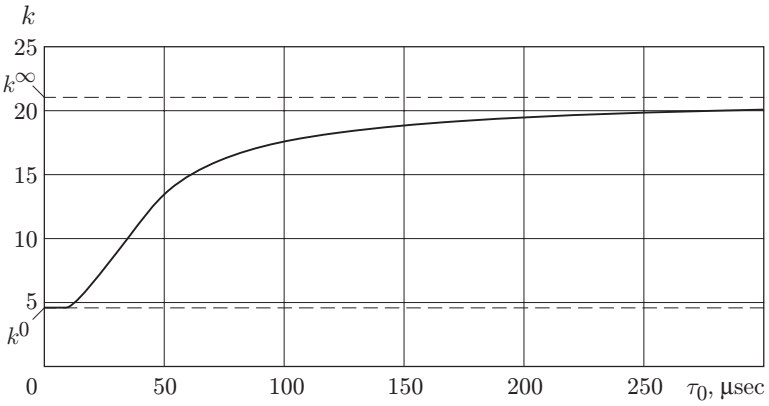

Fig. 6. Dependence $k(\tau_0)$.

with coordinates (σ_c, τ). For real materials, the indicated region has a certain extent, which corresponds to a certain range of loading time. Each loading times on the time curve of strength corresponds to a unique point with coordinates (P^*, t^*). Moving along the curve, one obtains the least amount of fracture $G_{\min}$, which corresponds to the minimum area of the rectangle P^*t^*.

3. Relation between Threshold Fracture Pulses for Materials with Different Internal Structure. The obtained threshold diagrams suggest that spall strength of materials depends greatly on the initial static fracture strength and the speed of elastic waves. The latter is determined by the elastic modulus and density of the material. The calculation results given above were obtained for different steel grades, i.e., for materials with crystalline structure. Let us investigate the behavior of the threshold fracture pulse for materials with significantly different internal structures, namely, for metals and polymers. As an example, we consider polymethylmethacrylate (PMMA) and AISI 4340 steel (Table 3). For PMMA, the incubation time was experimentally found in [12], and for AISI 4340 steel, in [13].

The threshold force pulse, strength, and incubation time for AISI 4340 steel will be denoted by U'_*, σ'_c, and τ', respectively, and the same characteristics for PMMA by U''_*, σ''_c, and τ'', respectively. Then, according to the expression for the threshold force pulse amplitude (2.1), the following relation holds:

$$k = \frac{U'_*}{U''_*} = \begin{cases} \sigma'_c\tau'/(\sigma''_c\tau'') \equiv k^0, & \tau_0 \to 0, \\ \sigma'_c/\sigma''_c \equiv k^\infty, & \tau_0 \to \infty; \end{cases} \tag{3.1}$$

here $\tau_0 = 2t_0$.

A curve of $k(\tau_0)$ is presented in Fig. 6. From the nature of this curve, one can see that on the static branch [the second expression in (3.1)], the relative strength of the materials considered is determined by the ratio of their static fracture strengths, and on the dynamic branch [the first expression in (3.1)], it is determined by the ratio of the products of the strength and the incubation time. In the limiting cases, we obtain $k^\infty = 21.3$ for $\tau_0 \to \infty$ and $k^0 = 4.7$ at $\tau_0 \to 0$. In other words, the difference between the strength properties of PMMA and AISI 4340 steel is much smaller under dynamic conditions than under static conditions.

Conclusions. The calculations of the time dependence of strength for rail steels of different grades indicate that steels having a high quasistatic fracture strength exhibit lower strength under high-speed impact loading, which is due to their lower fracture resistance. For a comprehensive comparative estimation of the spall strength of a material, it is expedient to use, as a criterion, the product of the threshold fracture amplitude and the time to fracture.

The analysis of the obtained diagrams suggests that the fracture intensity depends greatly on the initial static fracture strength and the speed of stress waves, which is determined by the elastic modulus and the density of the material. This implies that more rigid materials and materials with lower density have lower resistance to dynamic loading. The difference between the strength properties of materials with different internal structure (for example, metals and polymers) is smaller under rapid dynamic loading than under static loading.

REFERENCES

1. V. S. Nikiforovskii and E. I. Shemyakin, *Dynamic Fracture of Solids* [in Russian], Nauka, Novosibirsk (1979).
2. N. F. Morozov and Yu. V. Petrov, *Problems of Fracture Dynamics of Solids* [in Russian], Izd. St. Petersburg Univ., St. Petersburg (1997).
3. N. A. Zlatin, G. S. Pugachev, S. M. Mochalov, and A. M. Bragov, "Time dependence of the strength of metals for lifetimes of the microsecond range," *Fiz. Tverd. Tela*, **17**, No. 9, 2599–2602 (1975).
4. N. A. Zlatin, G. S. Pugachev, S. M. Mochalov, et al., "Time regularities of fracture under intense loads," *Fiz. Tverd. Tela*, **16**, No. 6, 1752–1755 (1974).
5. L. D. Volovets, N. A. Zlatin, and G. S. Pugachev, "Fracture kinetics of polymethylmethacrylate in a plane short wave of tensile stresses," in: *Problems of Strength and Plasticity of Solids* [in Russian], Nauka, Leningrad (1979), pp. 35–42.
6. Yu. I. Meshcheryakov, A. K. Divakov, and V. G. Kudryashev, "Dynamic strength with spalling and breakthrough," *Combust., Expl., Shock Waves*, No. 2, 241–248 (1988).
7. D. K. Nesterov, V. E. Sapozhkov, N. F. Levchenko, et al., "Structural strength and operational resistance of rails made of hypereutectoid steel and heat treated for high strength," in: *Transport: Science, Engineering, and Control* (collected scientific papers) [in Russian], No. 8, VINITI, Moscow (1991), 9–13.
8. "Manufacture of strengthened rails," *Zh. Zhelez. Dorogi Mira*, No. 11, 41–51 (1991).
9. S. E. Kovshik and E. M. Morozov, "Characteristics of short-term fracture resistance of materials and methods of their determination," in: *Fracture Mechanics and Strength of Materials* [in Russian], Vol. 3, Naukova Dumka, Kiev (1988).
10. A. N. Filin, N. A. Chelyshev, and V. N. Gul'nyashkin, "Mechanical characteristics of rail steel of experimental-commercial smelting," *Izv. Vyssh. Uchebn. Zaved., Chern. Metallurg.*, No. 2, 43–44 (1991).
11. Yu. V. Petrov, "On the 'quantum' nature of the dynamic fracture of brittle media," *Dokl. Akad. Nauk SSSR*, **321**, No. 1, 66–68 (1991).
12. A. N. Berezkin, S. I. Krivosheev, Yu. V. Petrov, et al., "Effect of a delay of crack start under threshold pulse loads," *Dokl. Ross. Akad. Nauk*, **375**, No. 3, 328–330 (2000).
13. H. Homma, D. A. Shockey, and Y. Murayama, "Response of cracks in structural materials to short pulse loads," *J. Mech. Phys. Solids*, **31**, No. 3, 261–279 (1983).